

# The Clustering of Little Red Dots from Ultra-Strongly Self-Interacting Dark Matter

M. Grant Roberts,<sup>1,2</sup>★ Aarna Garg,<sup>1</sup> Tesla Jeltema,<sup>1,2</sup> and Stefano Profumo<sup>1,2</sup>

<sup>1</sup>Department of Physics, University of California, Santa Cruz (UCSC), Santa Cruz, CA 95064, USA

<sup>2</sup>Santa Cruz Institute for Particle Physics (SCIPP), Santa Cruz, CA 95064, USA

Accepted XXX. Received YYY; in original form ZZZ

## ABSTRACT

We predict the effective clustering bias parameter,  $b_{\text{eff}}$ , at  $z \sim 5$  for Little Red Dots (LRDs) seeded by Ultra-Strongly Self-Interacting Dark Matter (uSIDM). From our model, we find that  $b_{\text{eff}} \sim 4.5$ , thus we infer that LRDs seeded by uSIDM would populate halos of typical masses  $\sim 8 \times 10^{10} M_{\odot}$ ; this bias factor is consistent with LRDs being a distinct population from high redshift quasars. To the extent that we are aware, this is the first formation-based theoretical prediction of LRD clustering from a model consistent with the LRD mass function. We find that this bias and clustering is insensitive to a wide range of the underlying uSIDM microphysics parameters, including the uSIDM cross-section  $\sigma/m$  and uSIDM fraction  $f$ . This is therefore a robust prediction from the uSIDM model, and will allow for direct probes of the uSIDM paradigm as the origin of LRDs in the next few years. Upcoming JWST observations will constrain the population of LRDs, including directly measuring their clustering.

**Key words:** dark matter – quasars: supermassive black holes – galaxies: luminosity function, mass function – galaxies: high-redshift – cosmology: theory

## 1 INTRODUCTION

Little Red Dots (LRDs) are a recently-discovered population of likely dust-enshrouded active galactic nuclei (AGN), most of which have redshifts in the range of  $4 < z < 7$ ; the corresponding super-massive black holes (SMBHs) are overmassive with respect to local black hole-galaxy scaling relations, and exhibit v-shaped spectral energy distributions, with a sharp Balmer break (Matthee et al. 2024; Kokorev et al. 2024; Greene et al. 2024; Kocevski et al. 2025). Given the highly compact nature of these objects ( $\lesssim 100$  parsec in size) in addition to the overmassive SMBHs, their existence raises the question of how such massive BHs formed so early in the universe. In particular, LRDs challenge standard models of early galaxy and black hole co-evolution, suggesting unusually rapid or non-standard growth channels at very early times. Moreover, current JWST observations increasingly constrain traditional baryonic seeding mechanisms (Volonteri 2010; Loeb & Rasio 1994; Inayoshi et al. 2020; Pacucci et al. 2017; Madau et al. 2014) due to these mechanisms having longer formation time scales, as well as tending to require large periods of super-Eddington accretion to make up for the initial seed formation delay.

As an alternative approach to seed formation, several papers have considered models of self-interacting dark matter (SIDM) leading to the formation of heavy seeds – either from dissipative effects (D’Amico et al. 2017; Latif et al. 2019; Choquette et al. 2019; Xiao et al. 2021; Shen et al. 2025; Buckley & Fernandez 2025) or through gravothermal evolution and the resulting core-collapse (Balberg & Shapiro 2002; Pollack et al. 2015; Feng et al. 2021; Outmezguine

et al. 2023; Gad-Nasr et al. 2024; Feng et al. 2025; Roberts et al. 2025c,a). In particular, ultra-strong self-interactions can rapidly accelerate the gravothermal process in very early halos to form much heavier BH seeds compared to baryonic seeding mechanisms.

In this Letter, we use the uSIDM model (Roberts et al. 2025c,a,b) to calculate the clustering of the population of LRDs that are seeded by the gravothermal core-collapse of uSIDM halos in the early universe. A possible underlying particle physics model for the uSIDM has been explicitly worked out in Roberts et al. (2025b). In short, the model consists of two dark matter particles: one is a standard DM candidate, possibly but not necessarily self-interacting, while the second one is the ultra-strongly self-interacting particle, which comprises only a small fraction of the dark matter. The mediator of the self interactions is a massive dark photon. The choice of one particle being ultra-strongly self-interacting ensures rapid gravothermal collapse and early seed formation prior to significant baryonic assembly, thereby providing a natural pathway toward overmassive black holes by  $z \sim 5$ .

Recent work has highlighted the need for observations and theoretical predictions of the clustering of LRDs (Arita et al. 2024; Lin et al. 2025; Schindler et al. 2025; Pizzati et al. 2025; Carranza-Escudero et al. 2025) which may help distinguish their origin; see Inayoshi & Ho (2025) for a recent review about LRDs. Arita et al. (2024) performed cross-correlation analysis of 27 low-luminosity broad-line AGNs with  $5 < z < 6$  and found characteristic mass scales of  $10^{11.46} h^{-1} M_{\odot}$ , which are around 1 dex smaller than luminous quasars at the same redshift. Lin et al. (2025) also looked at a sample of low-luminosity AGNs, and they found a characteristic mass scale of  $10^{11} M_{\odot} - 10^{11.2} M_{\odot}$ , which reinforces that these faint populations are hosted by more moderate size halos than luminous quasars. While

★ E-mail: mrober@ucsc.edu

both of these studies include significant overlap with LRDs, they do not perform a dedicated clustering or bias measurement for LRDs as a distinct population.

Further, Pizzati et al. (2025) ran mock-clustering simulations to infer potential LRD clustering measurements from JWST, and find that with  $\approx 10$  fields, they can constrain the characteristic halo mass scale of LRDs to within 0.1 – 0.3 dex. Thus, the accuracy needed to determine LRD clustering is within the reach of upcoming JWST surveys. Importantly, their mock results indicate the LRDs may be low-mass halos with modest duty cycles, raising the possibility that LRDs are a distinct population from quasars. On the other hand, Schindler et al. (2025) identified a single LRD at  $z \approx 7.3$  in an overdensity of eight nearby galaxies and inferred a correlation length of  $r_0 = 8 \pm 2 h^{-1}$  cMpc, which is consistent with ultraviolet luminous high-redshift quasars at  $z \approx 6$ . However, as this determination is based off of a single source, this cannot be a robust conclusion for the entire LRD population. Similarly, Carranza-Escudero et al. (2025) probed the local environments of LRDs by looking at a photometrically selected sample in  $3 < z < 10$ , and found evidence that LRDs tend to reside in less overdense local environments compared to galaxies of similar mass and redshift.

Together, these studies indicate the need for more LRD observations with JWST as well as for theoretical determinations of LRD clustering bias to determine the nature of these new objects. In this paper we tackle the latter issue and present the first theoretical calculation of LRD clustering. We assume a uSIDM seeding mechanism which can provide a critical test of heavy-seed formation scenarios.

The remainder of this paper is as follows: in the next section we summarize the uSIDM mechanism for early black hole formation; in sec. 3 we compute the effective halo bias; in the final sec. 4 we summarize and conclude.

## 2 USIDM PHENOMENOLOGY AND BLACK HOLE FORMATION

The uSIDM model for early SMBH formation (see Roberts et al. (2025b) for more details) is an extension of the typical SIDM model which also includes an additional, much more strongly self-interacting dark matter species comprising a small fraction,  $f$ , of the total dark matter budget. The governing Lagrangian is given by,

$$\begin{aligned} \mathcal{L}_{\text{dark}} = & \bar{\chi}_1 (i\cancel{\partial} - m_\chi) \chi_1 + \bar{\chi}_2 (i\cancel{\partial} - m_\chi) \chi_2 \\ & - g_{\chi_1 \bar{\chi}_1} A'^\mu \gamma_\mu \chi_1 - g_{\chi_2 \bar{\chi}_2} A'^\mu \gamma_\mu \chi_2 - \frac{1}{4} F'^{\mu\nu} F'_{\mu\nu} \\ & - \frac{1}{2} m_A'^2 A'^\mu A'_\mu, \end{aligned} \quad (1)$$

where  $\chi_1$  and  $\chi_2$  are the uSIDM and SIDM particle respectively, and  $A'$  is the dark photon. In order to have the onset of core-collapse occur shortly after our virialization redshift,  $z_{\text{vir}} \sim 13.5$ ,  $\chi_1$  couples much more strongly to the dark photon than  $\chi_2$ , i.e.,  $g_{\chi_1} >> g_{\chi_2}$ . This guarantees  $\chi_1$  to have a significantly enhanced cross-section. From previous uSIDM work (Roberts et al. 2025c), the uSIDM cross-section is on the order of  $10^4 \text{ cm}^2 \text{ g}^{-1}$  with a corresponding abundance fraction around  $10^{-3.5}$  in order to seed high-redshift black hole formation.

In Roberts et al. (2025a) we derived a LRD mass function from the uSIDM model at  $z_{\text{obs}} \sim 5$ , with a fixed duty cycle  $\varepsilon_{\text{DC}} = 0.01$  and a log-normal distribution of accretion rates based on Eddington ratios with mean  $\lambda_0 = 0.2$  and standard deviation  $\sigma_\lambda = 0.3$ , which we reproduce here in Fig. 1. In particular, we derived a “full mass” function and a “power-law” mass function. The full mass function

includes a toy BH merger model, an AGN duty cycle, and a luminosity cutoff matching observational constraints. The power-law mass function is a simple power-law fit of the form  $\phi_{\text{LRD}}(m_{\text{BH}}) = A m_{\text{BH}}^\alpha$ , where  $\log_{10} A$  and  $\alpha$  are our normalization and slope that we fit to our full model; this gives an analytic approximation to our full mass function. In Fig. 1, the colored points are the full mass function, whereas the solid and black dashed lines are the median and 1-sigma errors on the power-law fit.

While the duty cycle enters the number density normalization, the effective bias is independent of the duty cycle and is determined solely by the weighted halo mass distribution. Thus, the assumed value of  $\varepsilon_{\text{DC}}$  does not impact our clustering prediction. Similarly, for our uSIDM model, we do not require accretion at the Eddington limit to grow our BH seeds because uSIDM halos can collapse and form much heavier seeds; hence, modeling the Eddington ratios with a mean of  $\lambda_0 = 0.2$ , which is more typical of high-redshift AGN (Jiang et al. 2025; Xiao et al. 2021; Willott et al. 2010).

## 3 LRD CLUSTERING AND THE EFFECTIVE BIAS

The halo bias,  $b_h$ , is the relation between the two-point dark matter halo correlation function, and the two-point matter correlation function:  $\xi_{hh} \simeq b_h^2 \xi_{mm}$ . But since we are interested in a specific sub-population of dark matter halos as a tracer for LRDs, we need to calculate an effective bias. Therefore, we define the effective halo bias (Porciani et al. 2004; Fanidakis et al. 2013) as,

$$b_{\text{eff}} = \frac{\int d \log_{10} m_{200} N_{\text{LRD}} n(m_{200}) b_h[m_{200}, z]}{\int d \log_{10} m_{200} N_{\text{LRD}} n(m_{200})}, \quad (2)$$

where  $N_{\text{LRD}}$  is the mean number of LRDs that are hosted in halos of mass  $m_{200}$ ,  $n(m_{200})$  is the number density of DM halos with mass  $m_{200}$ , and  $b_h[m_{200}(m_{\text{BH}}), z]$  is the standard halo bias for which we use Tinker et al. (2010) via COLOSSUS (Diemer 2018). Equation (2) is given in terms of the halo mass, but under a change of variables, one can derive the effective bias in terms of the LRD mass function as a function of  $m_{\text{BH}}$ , instead of the halo mass function:

$$b_{\text{eff}} = \frac{\int d \log_{10} m_{200} \phi_{\text{LRD}}(m_{\text{BH}}) \frac{d \log_{10} m_{\text{BH}}}{d \log_{10} m_{200}} b_h[m_{200}, z]}{\int d \log_{10} m_{200} \phi_{\text{LRD}}(m_{\text{BH}}) \frac{d \log_{10} m_{\text{BH}}}{d \log_{10} m_{200}}}. \quad (3)$$

where  $\phi_{\text{LRD}}(m_{\text{BH}}) = dn_{\text{LRD}}/d \log_{10} m_{\text{BH}}$  is our LRD mass function, either the power-law fit or the full model. Physically, the effective bias is the number density weighted average quantity of the large scale LRD clustering strength. Since the halo bias is a monotonically increasing function with  $m_{200}$ ,  $b_{\text{eff}}$  is a direct probe of the underlying halo environment of LRDs.

We evaluate the mass integrals over the range of our BH masses from Fig. 1. To get a first approximation to  $b_{\text{eff}}$ , we use a power-law fit to  $\phi_{\text{LRD}}(m_{\text{BH}}) = A m_{\text{BH}}^\alpha$ , where we pick three fiducial values of  $\log_{10} A$  and  $\alpha$  that represent the solid black and dashed black gray lines in Fig. 1; specifically we use  $\{\log_{10} A, \alpha\} = \{2.22, -0.9\}$  for the central fit and  $\{\log_{10} A, \alpha\} = \{1.34, -0.92\}$  and  $\{0.27, -0.47\}$  for the 1-sigma range. These three fiducial parameter choices yield  $b_{\text{eff}} = (3.81, 3.86, 5.67)$ . These results are shown in Fig. 2, and we overlay the halo bias  $b_h[m_{200}(m_{\text{BH}}), z]$  from Tinker et al. (2010) in red. In order to determine the characteristic mass scale,  $m_{200}^{\text{char}}$ , for these values of  $b_{\text{eff}}$ , we numerically solve  $b_h[m_{200}^{\text{char}}(m_{\text{BH}}), z] = b_{\text{eff}}$ , and we find  $m_{200}^{\text{char}} = (3.67 \times 10^{10} M_\odot, 3.86 \times 10^{10} M_\odot, 1.82 \times 10^{11} M_\odot)$  for the three values of  $b_{\text{eff}}$  respectively. These three power-laws span

a large degree of the uSIDM parameter space, and thus the sensitivity to the slope of the LRD mass function and the implied characteristic mass scale. Therefore, even with a simple power-law fit, the implied  $m_{200}^{\text{char}}$  of LRDs fall on the low-to-moderate halo mass range compared to high-redshift luminous quasars as can be seen by the orange and blue bands which are the inferred mass ranges by the single LRD within an overdensity of eight galaxies in Schindler et al. (2025) and the mock-clustering simulations of JWST fields by Pizzati et al. (2025) respectively.

Equation (3) for  $b_{\text{eff}}$  works for a direct one to one mapping between  $m_{\text{BH}}$  and  $m_{200}$ , i.e., for a fixed  $\lambda_{\text{edd}}$ . But in general we sample from a log-normal distribution in  $\lambda_{\text{edd}}$ , thus we need to sample the integral. To do this, we employ a Monte Carlo procedure which samples from the distributions of  $m_{\text{BH}}$  and  $m_{200}$  for our full LRD mass function which includes the modeled distribution of accretion and merger histories. Specifically, we take  $N = N_{mc}$  samples with Monte Carlo weights  $w_i$  which randomly select from the final sample of BH masses and halo masses that survive the luminosity cutoff (see Roberts et al. (2025a) Section 3.2):

$$b_{\text{eff}} = \frac{\sum_i^{N_{mc}} w_i b_h[m_{200,i}, z]}{\sum_i^{N_{mc}} w_i}, \quad (4)$$

where  $w_i = w_0 \varepsilon_{\text{DC}}$  and  $w_0 = \frac{n_{\text{seed}}}{N_{mc}}$ , such that  $n_{\text{seed}}$  is the original number density of seeds:

$$n_{\text{seed}} = \int_{\log_{10} m_{200}^{\min}}^{\log_{10} m_{200}^{\max}} \frac{dN_{\text{Halo}}}{d \log_{10} m_{200}} d \log_{10} m_{200},$$

where  $\frac{dN_{\text{Halo}}}{d \log_{10} m_{200}}$  is the halo mass function, for which we use Tinker et al. (2008). Our mass range for the halos is  $10^{7.5} - 10^{11.5} M_{\odot}$  as these are in the range of most efficient core-collapse within uSIDM (Roberts et al. 2025c). In practice, this weighting procedure accounts for the intrinsic scatter in the black hole mass to halo mass relation introduced by our stochastic Eddington ratios. As a result, our full mass function clustering prediction incorporates a more realistic mapping between LRDs and their host halos.

In Fig. 3, we plot  $b_{\text{eff}}$  from our full mass function for each of the three examples in Fig. 1, for which we find  $b_{\text{eff}} = (4.54, 4.52, 4.49)$ . These three models were found in (Roberts et al. 2025a) to bracket the observed LRD mass function. From these values of  $b_{\text{eff}}$ , we find  $m_{200}^{\text{char}} \sim 8 \times 10^{10} M_{\odot}$  across our model curves. Given that  $b_{\text{eff}}$  is consistent to within 1%, this implies that the bias and hence characteristic mass of LRDs are relatively insensitive to the underlying particle physics, making this a robust prediction of the uSIDM scenario. This value of  $b_{\text{eff}}$  tells us that LRDs inherently are a different population than high-redshift quasars, which have a much larger bias and characteristic mass scale, as seen by the orange and blue regions in the figure. Therefore, our result is in tension with the mass scale derived in Schindler et al. (2025) - but is consistent with the low-mass and low-duty cycle forecast performed by Pizzati et al. (2025) and the faint AGNs analyzed by Arita et al. (2024) and Lin et al. (2025).

#### 4 SUMMARY AND CONCLUSIONS

In this Letter, we use a model for the LRD mass function resulting from early core-collapse in scenarios where a fraction of the dark matter is ultra-strongly self-interacting to calculate the effective clustering bias,  $b_{\text{eff}}$ , and characteristic mass scale,  $m_{200}^{\text{char}}$ , of LRDs seeded by uSIDM. We find that both an approximate power law fit to the

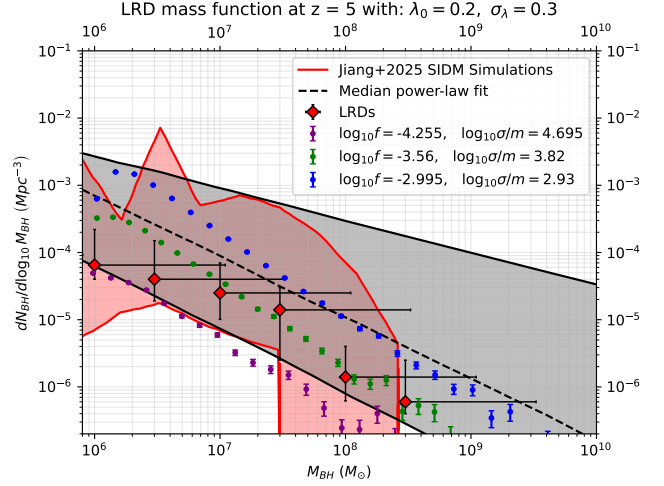


**Figure 1.** Here we reproduce Fig. 2 (right) from Roberts et al. (2025a). The uSIDM LRD mass function (colored dots) for different uSIDM parameters is shown. The uSIDM results are plotted against the SIDM simulation results from Jiang et al. (2025) (shaded red), and the LRD mass function data points from Kokorev et al. (2024) (red diamonds). The red diamonds are the derived BH masses, assuming  $\lambda_{\text{Edd}} = 1$ ; for lower accretion rates these would shift to larger BH masses as depicted by the horizontal lines which extend down to  $\lambda_{\text{Edd}} = 0.1$ . The simulations for the red shaded region assume  $\varepsilon_{\text{DC}} = 1$  whereas we assume  $\varepsilon_{\text{DC}} = 0.01$ .

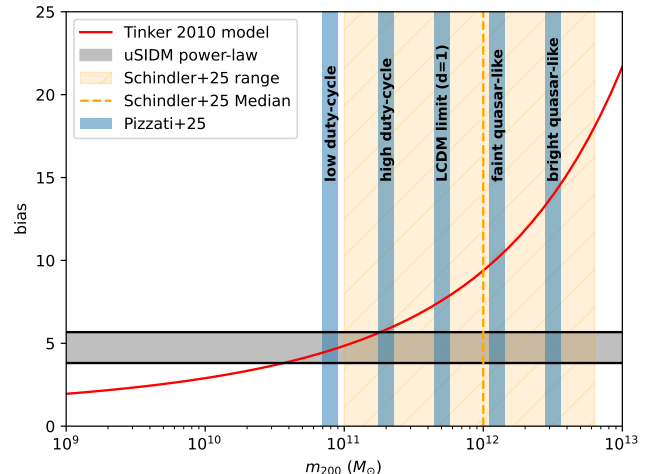


**Figure 2.** Here we show the range of  $b_{\text{eff}}$  from the three power-law fits to the uSIDM LRD mass function,  $3.81 \lesssim b_{\text{eff}} \lesssim 5.67$  (gray shaded region), overlaid onto the Tinker et al. (2010) halo bias function (red line). We find a rough scale for  $m_{200}^{\text{char}}$  to be  $(0.4 - 1.8) \times 10^{11} M_{\odot}$ . We also show the inferred mass range from Schindler et al. (2025) in shaded orange, with the median inferred value as the dashed orange vertical line. In blue we plot the various cases explored by Pizzati et al. (2025).

mass function and a full Monte Carlo sampling of the astrophysical parameters (the accretion and merger rates) are in rough agreement with the predicted LRD clustering. We also find that  $b_{\text{eff}}$  is insensitive to the underlying particle physics, and hence, our model predictions are robust across the relevant parameter space. While it does not directly constrain the underlying particle parameters,  $b_{\text{eff}}$  is a uniform, consistent prediction from generic uSIDM seeding LRD formation,

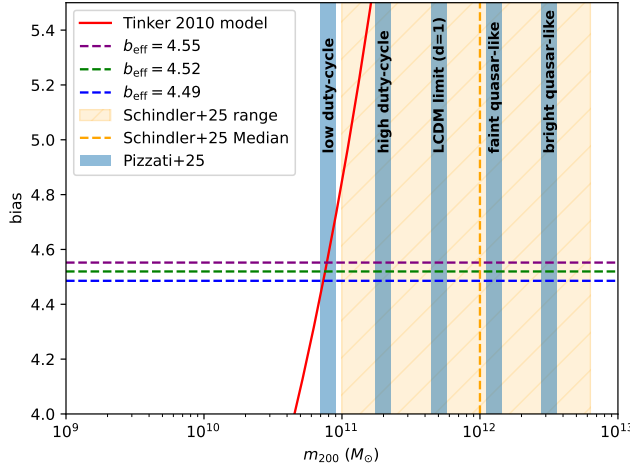


**Figure 3.** Here we show  $b_{\text{eff}}$  from the three representative full uSIDM LRD mass function curves. We find that the full mass function yields  $b_{\text{eff}}$  values that are very nearly insensitive to the underlying particle physics. They all yield  $b_{\text{eff}} \sim 4.5$  and thus  $m_{200}^{\text{char}} \sim 8 \times 10^{10} M_{\odot}$ . To show the small deviations in  $b_{\text{eff}}$ , we zoom into bias values between 4 and 5.5. As in Fig. 2, we plot the inferred mass regions from Schindler et al. (2025) in orange and Pizzati et al. (2025) in blue. We find that we are consistent with the low mass and low duty cycle case in Pizzati et al. (2025).

and is thus an excellent observational test of this model. Based on the uSIDM value of  $b_{\text{eff}} \sim 4.5$  and hence  $m_{200}^{\text{char}} \sim 8 \times 10^{10} M_{\odot}$ , we infer that LRDs in this scenario would represent a distinct population inhabiting lower-mass halos than high-redshift quasars. Thus, our model predictions are consistent with characteristic masses inferred by faint AGN analysis by Arita et al. (2024) and Lin et al. (2025), as well as the low-mass low-duty cycle scenario explored by Pizzati et al. (2025). This distinct prediction is falsifiable and therefore constitutes a clear observational test of the uSIDM seeded LRD formation scenario and can be tested with upcoming JWST surveys. This is, to our knowledge, the first quantitative prediction of the clustering of LRDs, from a formation scenario that maps consistently onto the LRD mass function.

While we have focused on uSIDM seeded LRD formation, it is worth emphasizing that different physical production mechanisms of BH seeds generically predict different values for  $b_{\text{eff}}$ , due to their distinct assumptions about the mapping between black hole mass and host halo mass, including effects from the concentration-mass relation, uncertainties on initial seed masses, and the subsequent growth history, which together determine the  $m_{\text{BH}}$  to  $m_{200}$  relation. A systematic comparison of  $b_{\text{eff}}$  predictions across different LRD formation channels is therefore an important and exciting avenue for future theoretical work.

In light of this, while our model produces an initial prediction, we can generalize the uSIDM model to include other effects to refine the predicted LRD number densities and the uSIDM  $m_{\text{BH}} - m_{200}$  relation, such as adding dark Bondi accretion to our seed growth (Feng et al. 2025), testing different log-normal distributions for Eddington accretion rates, different duty cycles, different luminosity cut offs, different BH merger scenarios, and N-body simulations of uSIDM. These extensions may allow us to model LRD growth and abundance more self-consistently, and potentially tighten the mapping between BH and halo mass. With these future refinements, we may also be able to predict the clustering redshift evolution as more LRDs are found at different redshifts. Because LRD clustering is a tracer for

early BH formation, growth, and feedback, these measurements may help us to discriminate between heavy and light seed scenarios, and thereby give insight to the physical origin of LRDs.

## ACKNOWLEDGEMENTS

This work is partly supported by the U.S. Department of Energy grant number de-sc0010107 (SP).

## DATA AVAILABILITY

No new data were generated or analyzed in support of this research.

## REFERENCES

Arita J., Kashikawa N., Onoue M., Yoshioka T., Takeda Y., Hoshi H., Shimizu S., 2024, *Monthly Notices of the Royal Astronomical Society*, 536, 3677  
 Balberg S., Shapiro S. L., 2002, *Phys. Rev. Lett.*, 88, 101301  
 Buckley M. R., Fernandez N., 2025, *J. Cosmology Astropart. Phys.*, 2025, 085  
 Carranza-Escudero M., et al., 2025, *ApJ*, 989, L50  
 Choquette J., Cline J. M., Cornell J. M., 2019, *J. Cosmology Astropart. Phys.*, 2019, 036  
 D'Amico G., Panci P., Lupi A., Bovino S., Silk J., 2017, *Monthly Notices of the Royal Astronomical Society*, 473, 328  
 Diemer B., 2018, *ApJS*, 239, 35  
 Fanidakis N., et al., 2013, *Mon. Not. Roy. Astron. Soc.*, 435, 679  
 Feng W.-X., Yu H.-B., Zhong Y.-M., 2021, *ApJ*, 914, L26  
 Feng W.-X., Yu H.-B., Zhong Y.-M., 2025, *arXiv e-prints*, p. arXiv:2506.17641  
 Gad-Nasr S., Boddy K. K., Kaplinghat M., Outmezguine N. J., Sagunski L., 2024, *J. Cosmology Astropart. Phys.*, 2024, 131  
 Greene J. E., et al., 2024, *The Astrophysical Journal*, 964, 39  
 Inayoshi K., Ho L. C., 2025, *arXiv e-prints*, p. arXiv:2512.03130  
 Inayoshi K., Visbal E., Haiman Z., 2020, *ARA&A*, 58, 27  
 Jiang F., Jia Z., Zheng H., Ho L. C., Inayoshi K., Shen X., Vogelsberger M., Feng W.-X., 2025, *arXiv e-prints*, p. arXiv:2503.23710  
 Kocevski D. D., et al., 2025, *ApJ*, 986, 126  
 Kokorev V., et al., 2024, *The Astrophysical Journal*, 968, 38  
 Latif M. A., Lupi A., Schleicher D. R. G., D'Amico G., Panci P., Bovino S., 2019, *MNRAS*, 485, 3352  
 Lin X., et al., 2025, *arXiv e-prints*, p. arXiv:2505.02896  
 Loeb A., Rasio F. A., 1994, *ApJ*, 432, 52  
 Madau P., Haardt F., Dotti M., 2014, *The Astrophysical Journal Letters*, 784, L38  
 Matthee J., et al., 2024, *ApJ*, 963, 129  
 Outmezguine N. J., Boddy K. K., Gad-Nasr S., Kaplinghat M., Sagunski L., 2023, *Mon. Not. Roy. Astron. Soc.*, 523, 4786  
 Pacucci F., Natarajan P., Volonteri M., Cappelluti N., Urry C. M., 2017, *ApJ*, 850, L42  
 Pizzati E., Hennawi J. F., Schaye J., Eilers A.-C., Huang J., Schindler J.-T., Wang F., 2025, *Monthly Notices of the Royal Astronomical Society*, 539, 2910  
 Pollack J., Spergel D. N., Steinhardt P. J., 2015, *ApJ*, 804, 131  
 Porciani C., Magliocchetti M., Norberg P., 2004, *Mon. Not. Roy. Astron. Soc.*, 355, 1010  
 Roberts M. G., Braff L., Garg A., Profumo S., Jeltema T., 2025a, *arXiv e-prints*, p. arXiv:2507.03230  
 Roberts M. G., Altmannshofer W., Giffin P., Profumo S., 2025b, *arXiv e-prints*, p. arXiv:2510.18142  
 Roberts M. G., Braff L., Garg A., Profumo S., Jeltema T., O'Donnell J., 2025c, *J. Cosmology Astropart. Phys.*, 2025, 060  
 Schindler J.-T., et al., 2025, *Nature Astronomy*, 9, 1732

Shen T., Shen X., Xiao H., Vogelsberger M., Jiang F., 2025, [arXiv e-prints](#), p. [arXiv:2504.00075](#)

Tinker J. L., Kravtsov A. V., Klypin A., Abazajian K., Warren M. S., Yepes G., Gottlöber S., Holz D. E., 2008, *The Astrophysical Journal*, 688, 709

Tinker J. L., Robertson B. E., Kravtsov A. V., Klypin A., Warren M. S., Yepes G., Gottlöber S., 2010, *ApJ*, 724, 878

Volonteri M., 2010, *The Astronomy and Astrophysics Review*, 18, 279–315

Willott C. J., et al., 2010, *The Astronomical Journal*, 140, 546

Xiao H., Shen X., Hopkins P. F., Zurek K. M., 2021, *Journal of Cosmology and Astroparticle Physics*, 2021, 039

This paper has been typeset from a  $\text{\TeX}/\text{\LaTeX}$  file prepared by the author.